

# Sedimentary facies and Holocene progradation rates of the Changjiang (Yangtze) delta, China

Kazuaki Hori <sup>a,\*</sup>, Yoshiki Saito <sup>b</sup>, Quanhong Zhao <sup>c</sup>, Xinrong Cheng <sup>c</sup>,  
Pinxian Wang <sup>c</sup>, Yoshio Sato <sup>d</sup>, Congxian Li <sup>c</sup>

<sup>a</sup> *Department of Earth and Planetary Science, Graduate School of Science, University of Tokyo, Hongo 7-3-1, Bunkyo, Tokyo 113-0033, Japan*

<sup>b</sup> *MRE, Geological Survey of Japan, AIST, Central 7, Higashi 1-1-1, Tsukuba, Ibaraki 305-8567, Japan*

<sup>c</sup> *Laboratory of Marine Geology, Tongji University, Shanghai, 200092, PR China*

<sup>d</sup> *Geology Department, Science Faculty, Chulalongkorn University, Phya Thai Road, Bangkok, Thailand*

Received 27 February 2000; received in revised form 20 August 2000; accepted 2 June 2001

## Abstract

The Changjiang (Yangtze) River, one of the largest rivers in the world, has formed a broad tide-dominated delta at its mouth during the Holocene sea-level highstand. Three boreholes (CM97, JS98, and HQ98) were obtained from the Changjiang delta plain in 1997–1998 to clarify the characteristics of tide-dominated delta sediments and architecture. Based on sediment composition and texture, and faunal content, core sediments were divided into six depositional units. In ascending order, they were interpreted as tidal sand ridge, prodelta, delta-front, subtidal to lower intertidal flat, upper intertidal flat, and surface soil deposits. The deltaic sequence from the prodelta deposits to the delta front deposits showed an upward-coarsening succession, overlain by an upward-fining succession from the uppermost part of the delta front deposits to the surface soil. Thinly interlaminated to thinly interbedded sand and mud (sand–mud couplets), and bidirectional cross laminations in these deposits show that tide is the key factor affecting the formation of Changjiang deltaic facies. Sediment facies and their succession combined with AMS <sup>14</sup>C dating revealed that isochron lines cross unit boundaries clearly, and delta progradation has occurred since about 6000 to 7000 years BP, when the rising sea level neared or reached its present position. The average progradation rate of the delta front was approximately 50 km/kyear over the last 5000 years. The progradation rate, however, increased abruptly ca. 2000 years BP, going from 38 to 80 km/kyear. The possible causes for this active progradation could have been an increase in sediment production in the drainage basin due to widespread human interference and/or decrease in deposition in the middle reaches related to the channel stability caused by human activity and climatic cooling after the mid-Holocene. © 2001 Elsevier Science B.V. All rights reserved.

*Keywords:* Progradation; Tide-dominated delta; Sea-level change; Changjiang (Yangtze) River; Sediment discharge

## 1. Introduction

Delta progradation has occurred in many places during the Holocene sea-level highstand, mainly during the last 8500 to 6500 years (Stanley and Warne, 1994). Tides and waves modify and affect the delta's

\* Corresponding author. Tel.: +81-298-61-3709; fax: +81-298-61-3747.

*E-mail address:* k-hori@aist.go.jp (K. Hori).

shape, development, and sediment dynamics (Galloway, 1975). Subsidence is also important in determining delta plain environments and delta facies architecture (Stanley, 1988). However, sediment discharge is the fundamental process in delta evolution (Coleman, 1981).

Asian rivers used to contribute more than 40% of total world sediment discharge shortly before the proliferation of dam construction in the latter half of this century (Milliman, 1991). However, this disproportionate contribution is considered to be not the natural state, but the result of widespread human activities, such as farming and deforestation for the last 2000 to 3000 years (Milliman and Syvitski, 1992). The study of past sediment discharge and its change over time of Asian rivers is of great importance to the better understanding of global changes.

The Changjiang (Yangtze) River is one of the largest rivers in the world in terms of suspended sediment load, water discharge, length, and drainage area. The river has formed a broad tide-dominated delta at its mouth since 6000 to 7000 years BP

(Wang et al., 1981; Li and Li, 1983) when sea level reached or approached its present level (Zhao et al., 1979; Chen et al., 1985b; Chen and Stanley, 1998).

Based on evidence from archeological sites, historical records, and  $^{14}\text{C}$  ages, Wang et al. (1981) estimated that the progradation rate of the main part of the subaerial delta plain began to increase at about 2000 years BP. The accelerated expansion of the southern delta plain since 2000 years BP has also been reported by studies of the chenier plain (Chen et al., 1985a; Chen, 1996). These studies, however, lack  $^{14}\text{C}$  ages from the subsurface delta deposits which constitute the main part of the delta, and therefore do not provide a complete picture of the Holocene Changjiang delta progradation.

The objective of this paper is to describe the characteristics of the Changjiang delta sediments in detail, define the facies architecture, and determine progradation rates of the delta, based on sedimentary facies analysis and AMS  $^{14}\text{C}$  dating of samples from three boreholes recovered from the central Changjiang delta plain (Fig. 1).

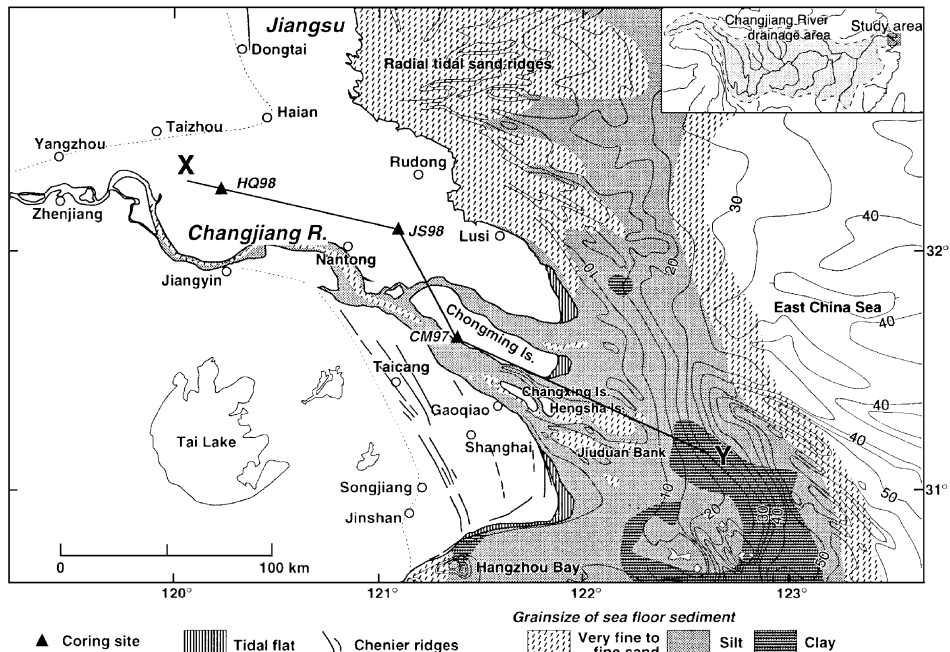


Fig. 1. Map showing the study area, bathymetry, distribution of sea-floor sediments and chenier ridges. Water-depth contour interval is 5 m. The distribution of chenier ridges is after Liu and Walker (1989) and Yan et al. (1989). Surface sediment data are after Department of Marine Geology, Tongji University (1975), Li et al. (1983), and Li (1986). Bathymetric data are after Editorial Board for Marine Atlas (1990). X–Y is the longitudinal cross section shown in Fig. 6.

## 2. Study area

The Changjiang River, which has a drainage area of 1.80 million km<sup>2</sup>, is the fourth and fifth largest in the world in terms of suspended load (480 million tons/year) and water discharge (921 km<sup>3</sup>/year), respectively (Milliman and Meade, 1983). About 70% of the annual water discharge occurs during flood season (May to October). The sediment discharge during flood season constitutes 87.2% of the annual sediment load. Most of the suspended sediments are silts and clays (Shen et al., 1988).

The present mean tidal range is 2.7 m near the river mouth, and the maximum tidal range approaches 4.6 m (Shen et al., 1988). Annually, the tidal current reaches an average of 210 km upstream from the river mouth (Shen, 1998). The tidal-current limit moves downstream from the average position about 30 km during the flood season and upstream about 80 km during the dry season (Shen, 1998). The mean and maximum wave heights at the river mouth are 0.9 and 6.2 m, respectively. The waves are mainly wind-driven waves, and secondly swell. The wind-driven waves approach the coast mainly from the north in winter and from the south direction in

summer (Zhu et al., 1988). According to the shore-line classification system of Davis and Hayes (1984), the Changjiang River mouth area should be plotted near the boundary between a tide-dominated and a mixed energy coast.

The Changjiang delta is classified as a typical tide-dominated mud delta (Orton and Reading, 1993) with a funnel-shaped topography and several wide distributary channels or estuaries (Fig. 1). The delta occupies an area of approximately 52,000 km<sup>2</sup>, 23,000 km<sup>2</sup> subaerial and 29,000 km<sup>2</sup> subaqueous (Li, 1986). The elevation of the delta plain is usually less than 5 m above mean sea level (Stanley and Chen, 1996; Chen, 1999). The main delta plain was formed by the step-like seaward migration (Fig. 2) of the river-mouth sand bars from Zhenjiang, the apex of the delta, to the present river mouth (Wang et al., 1981; Li and Li, 1983; Li et al., 2000a), or by a more complicated migration (Chen et al., 1985a). The main part of the delta is located over the incised valley formed by the paleo-Changjiang River during the last glacial period. Several chenier ridges composed of well-sorted fine sand and shell fragments are recognized in the southern part of the delta plain (Liu and Walker, 1989; Yan et al., 1989). Muddy

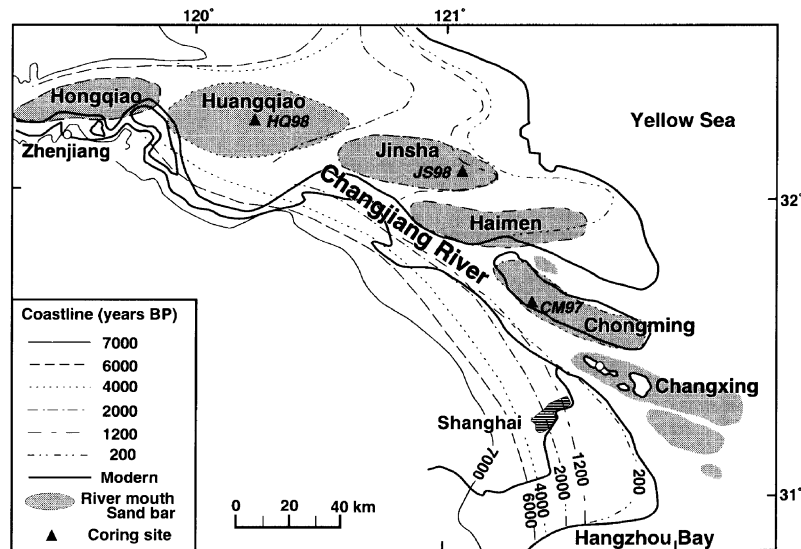


Fig. 2. Estimated evolution of Holocene coastlines and river-mouth sand bars in the Changjiang River delta during the last 7000 years. After Li and Li (1983) and Liu et al. (1992).

intertidal flats are developed extensively along the east coast of the delta plain with an average growth rate of 20 m/year presently (Chen, 1998).

River-mouth sand bars of the present Changjiang delta are elongated and oriented in the same direction as the river channel. There are three active sand bars in the river-mouth area extending southeastward. Temporal changes in bathymetry, shallower than about 10 m, indicate seaward migration of the subaqueous parts of these sand bars (Chen et al., 1982).

The subaqueous part of the delta can be divided into three parts: subtidal flats less than 5 to 10 m in water depth; delta front at water depths ranging from 5–10 to approximately 15–30 m; and prodelta at depths greater than 15 to 30 m. The slope of the delta front is from 0.0006 to 0.001 (Chen et al., 1987). The present delta is prograding southeastward and downlapping onto the paleo-Changjiang incised valley, which formed in the inner shelf of the East China Sea during the sea-level lowstand of the last glacial period (Chen et al., 1987). Strong tidal currents form radial tidal sand ridges off the Jiangsu Province coast north of the Changjiang delta. The sediments constituting these ridges are supplied mainly from the marginal parts of the radial ridges and the abandoned Yellow River delta (Liu et al., 1989).

### 3. Materials and methods

Three boreholes 10 cm in diameter were obtained from the present delta plain by rotary drilling in 1997–1998: CM97 (lat. 31°37'N, long. 121°23'E, elevation 2.48 m, penetration depth 70 m), JS98 (lat. 32°05'N, long. 121°05'E, elevation 4.20 m, penetration depth 60 m), and HQ98 (lat. 32°15'N, long. 120°14'E, elevation 5.91 m, penetration depth 60 m). Core recovery was more than 80%. The upper 25 to 30 m of each borehole is discussed in this paper.

These sediment cores were split, described, and photographed. X-radiographs were taken using slab samples (5 or 6 cm wide × 20 or 25 cm long × 1 cm thick) from all split cores. Sand and mud contents were measured in 5-cm-thick samples collected at 20-cm intervals by using 4.0 phi sieve.

Thirty-two  $^{14}\text{C}$  ages were obtained on molluscan shells and plant materials from the upper parts of the cores by Beta Analytic (Lab No. Beta) by using Accelerator Mass Spectrometry (AMS). Age determinations were based on a Libby half-life of 5568 years.  $^{14}\text{C}$  ages used in this paper were not corrected for isotopic fractionation based on the measured  $^{13}\text{C}/^{12}\text{C}$  ratio so that the accumulation curves at each site could be compared with known sea-level curves in the East China Sea.

### 4. Results

Borehole sediments can be divided into six depositional units, A to F, from bottom to top of the core on the basis of sedimentary facies (Fig. 3). Thickly interlaminated to thinly interbedded sand and mud (sand–mud couplets) are common in Units A, C, D, and E. Therefore, we first describe the characteristics of the sand–mud couplets. Afterwards, Units A to F are described individually and interpreted, and finally  $^{14}\text{C}$  ages and sediment accumulation rate of the core sediments are discussed.

#### 4.1. Description of sand–mud couplets

Sand–mud couplets in the upper part of core sediments are classified into six types, Types a to f, based on sedimentary textures, lithology, and physical sedimentary structures (Fig. 4). The characteristics of these six types are described below.

Type a (Fig. 4a) couplets are characterized by an upward-thinning succession, in which the mud layers become dominant upward. Most sand layers have relatively sharp, nonerosional contacts with the underlying and overlying mud layers. The thickness of a single couplet is between 3 and 40 mm. The sand layers are composed of well-sorted silty to fine sand. The thickness of the sand layers ranges from 1 to 30 mm. Ripple laminations are common in sand layers. Some layers show bidirectional ripple laminations. The mud layers typically consist of silty clay, 1 to 10 mm thick. Some may have been amalgamated. Organic matter composed of plant fragments commonly occurs in mud layers.

Type b (Fig. 4b) couplets are sand-dominant with transitional boundaries between sand and mud. A single couplet ranges from 4 to 25 mm in thickness.

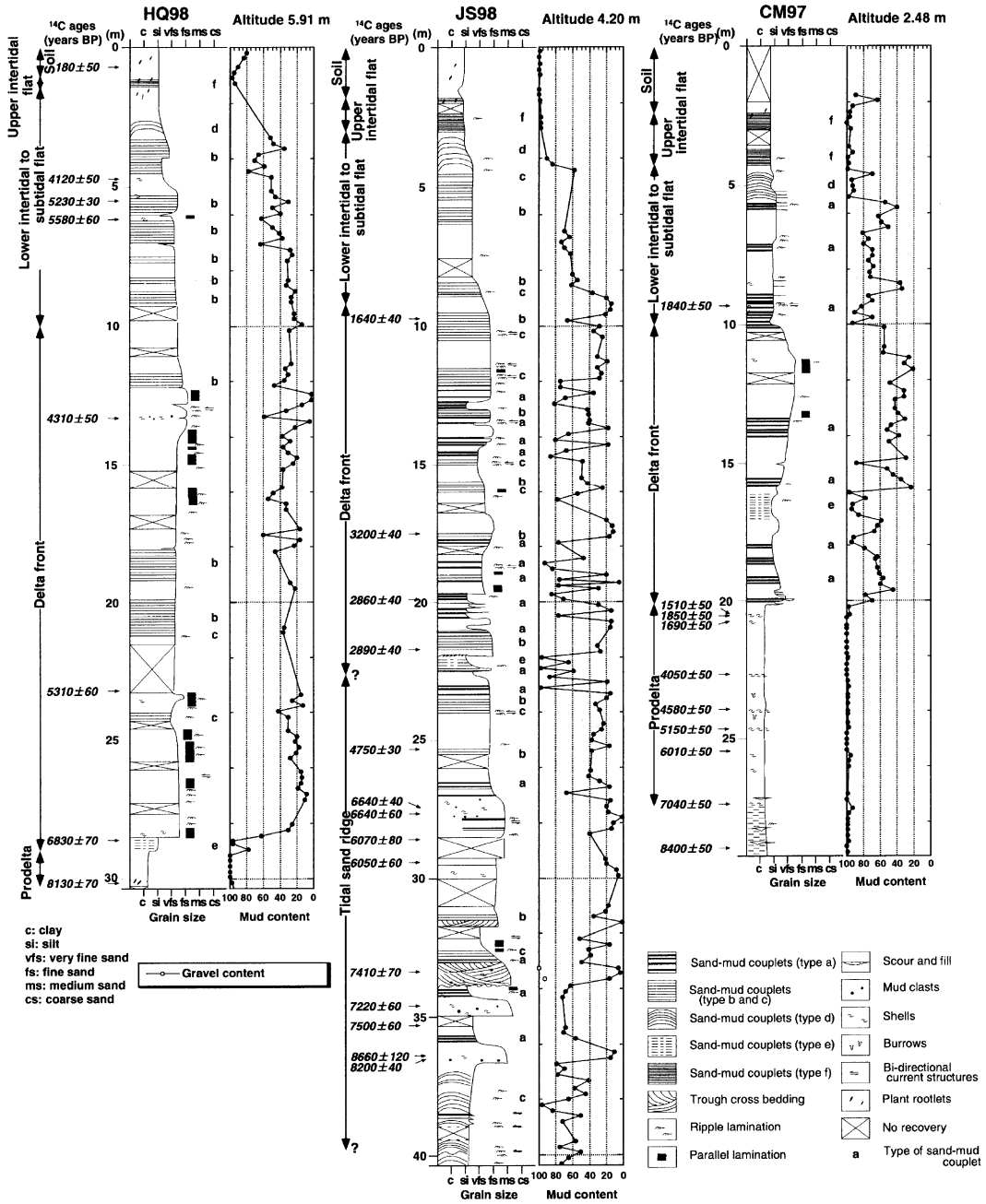


Fig. 3. Geological column of each borehole.

Sand layers consist of well-sorted very fine to fine sand. The thickness of the sand layers ranges from 3 to 22 mm. Sedimentary structures in sand layers are not clear. Mud layers are 1 to 5 mm thick and

composed of silt. Nearly invisible, very thin sand layers commonly occur in thick mud layers. Successions of this type are analogous to flaser bedding (Reineck and Wunderlich, 1968).

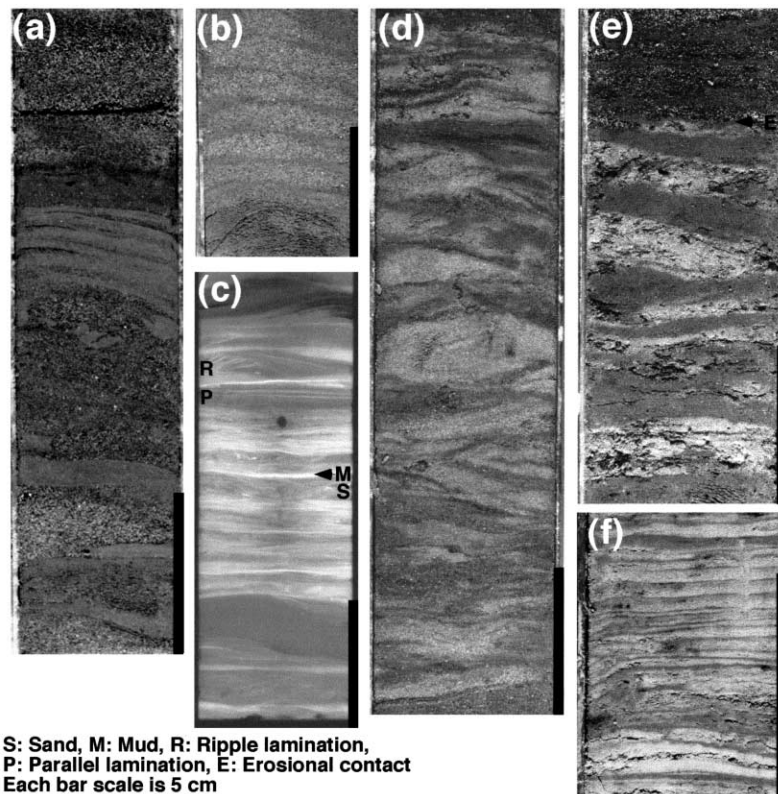


Fig. 4. Photographs and an X-radiograph of Type a to Type f sand–mud couplets. (a) Type a couplets: CM97, 9.05–9.25 m depth. (b) Type b couplets: HQ98, 5.50–5.75 m depth. (c) Type c couplets: JS98, 11.75–12.00 m depth. Ripple and parallel laminations in the sand layers can be recognized by X-radiograph. (d) Type d couplets: JS98, 4.20–4.45 m depth. (e) Type e couplets: JS98, ca. 21.75–22.00 m depth. An erosional contact with overlying type b couplets is visible. (f) Type f couplets: JS98, ca. 1.90–2.00 m depth. Plant rootlets are visible.

Type c couplets (Fig. 4c) are also sand-dominant and are characterized by ripple or parallel laminations in the sand layers. Some ripple laminations are bidirectional. Other characteristics are almost same with Type b.

Type d couplets (Fig. 4d) are characterized by ripple laminations in sand layers. Some sand layers display offshoot structures. The boundaries between sand and mud layers are transitional. Each couplet is generally less than 20 mm thick. Sand layers are composed of silty to very fine sand, and mud layers of silt to silty clay. These characteristics show that the sand layers formed wave ripples.

Type e couplets (Fig. 4e) are characterized by thick mud layers. However, the mud layers are sometimes amalgamated or intercalated with very thin sand laminations. Most of the boundaries between

sand and mud layers are sharp and not erosional. Sand layers are composed mainly of silty sand. The thickness of the sand layers ranges from 3 to 35 mm. Ripple laminations occasionally occur in sand layers. Mud layers consist of silty clay that range from 3 to 18 mm in thickness.

Type f couplets (Fig. 4f) have the very thin single sand–mud couplet thickness generally less than 3 mm and contain plant rootlets and fragments. Both the upper and lower boundaries of the sand layers are occasionally sharp. Sand layers less than 3 mm thick are composed of coarse silt to very fine sand. Ripple laminations are occasionally observed in the sand layers. Mud layers less than 2 mm thick consist mainly of silt.

In general, the formation of these sand–mud couplets is related to the alternation of current or wave

action and slack water (Reineck and Wunderlich, 1968). Bidirectional ripple laminations strongly suggest that flood and ebb tides formed these structures.

#### 4.2. Characteristics of depositional units and their interpretation

##### 4.2.1. Unit A (tidal sand ridge)

Unit A was observed only in JS98. It is ~15 m thick, but the boundary between the base of the unit and the underlying sediments was not clear. The unit consists mainly of several sets of an upward-fining succession composed of poorly sorted very fine to medium sand, overlain by thickly interlaminated to thinly interbedded sand and mud (sand–mud couplets). The thickness of each set is less than 2 m. The poorly sorted very fine to medium sand contains abundant molluscan shell fragments and mud clasts, and occasionally shows trough-cross bedding. Very thin to thin beds of mud are commonly intercalated in the fine to medium sand at 27.8 to 28.5 m depth. Sand–mud couplets recognized in the unit are Types a, b, c, and d.

Unit A probably represents a tidal sand-ridge environment because the characteristics of the unit are similar to those of tidal sand-ridge deposits in the North Sea and the Yellow Sea (Houbolt, 1968; Park and Lee, 1994; Lee and Yoon, 1997). The poorly sorted sand with shell fragments and mud clasts are interpreted as lag deposits in the swales between ridges (Houbolt, 1968).

Strong tidal currents rework sandy sediments on the East China Sea continental shelf and maintain the present radial tidal sand ridges off Jiangsu Province (Liu et al. 1989). The large number of sand deposits in this unit would also be supplied from the continental shelf, as shown by the present tidal sand ridges.

##### 4.2.2. Unit B (prodelta)

Unit B is composed of dark-gray silty clay with thin shell beds and coarse-silt layers. The thickness of the unit is 7.2 m in CM97 and 1.5 m in HQ98. This unit is not recognized in JS98. The unit has a gradational contact with underlying deposits. Its sediments had the finest grain size of all units, and mud content was generally over 95%. The coarse silt layers showing parallel and cross laminations are

commonly associated with small-scale cut-and-fill structures. Marine molluscan shells, such as *Bornioopsis tsurumaru* (Habe), are common. Burrows filled with coarse silt occur in CM97.

These features indicate that the unit was deposited under a low-energy prodelta environment (Coleman and Wright, 1975; Coleman, 1981). Storm currents would explain the scour-and-fill structures filled with coarse silt and episodic shell layers (Xu et al., 1990).

##### 4.2.3. Unit C (delta front)

Unit C is characterized by an upward-coarsening succession. Sand content is high relative to other units. The sediments in CM97 and JS98 consist of dark-gray silty to fine sand and thickly interlaminated to thinly interbedded sand and mud (sand–mud couplets). In contrast, well-sorted very fine to fine sand containing few shell fragments is predominant in HQ98. The sand shows ripple and parallel laminations. Bidirectional ripple laminations and herringbone structures occur intermittently. The upper part of this unit is the coarsest found in any of the six units except for the sand-ridge sediments. The base of the unit has a sharp contact with the underlying Unit B in CM97 and HQ98, but the contact was not clear in JS98. The thickness of this unit is 10.1 m in CM97, 13.3 m in JS98, and 19.0 m in HQ98.

Types a, b, c, and e couplets are found in this unit. Type a couplets commonly occur in CM97 and JS98. Type b couplets occur occasionally in JS98 and are predominant from 18 to 21 m depth in HQ98. Type c couplets are recognized in the upper part of JS98 and are occasionally observed in HQ98. Type e couplets occur in the lowermost part of the unit in JS98 and HQ98, and in the lower part of the unit in CM97. The top of one couplet is obviously eroded prior to deposition of a Type b couplet in JS98 (Fig. 4e).

As upward-coarsening successions are common in delta front deposits (Coleman and Wright, 1975) and, as the coarsest part, may correspond to river-mouth sand-bar deposits (Coleman, 1981), Unit C is interpreted as delta front facies strongly influenced by tides.

##### 4.2.4. Unit D (lower intertidal to subtidal flat)

Unit D showing an upward-fining succession is characterized by thickly interlaminated to thinly in-

Table 1  
<sup>14</sup>C ages of core sediments

Sample no.	Altitude (m)	Material	Species	Weight (mg)	<sup>14</sup> C age (years BP)	δ <sup>13</sup> C (‰)	Conventional <sup>14</sup> C age (years BP)	Code no. (Beta)
<i>CM97</i>								
CM-A7-931	−6.83	Molluscan shell	<i>B. ariakensis</i> Habe	21	1840 ± 50	−7.0	2140 ± 50	117615
CM-B20-2048	−18.00	Molluscan shell	<i>B. ariakensis</i> Habe	14	1510 ± 50	−6.0	1830 ± 50	120476
CM-B20-2053	−18.05	Molluscan shell	<i>B. ariakensis</i> Habe	30	1850 ± 50	−7.6	2130 ± 50	120477
CM-B20-2073	−18.25	Molluscan shell	<i>Nemocardium</i> sp.	34	1690 ± 50	−7.6	1970 ± 50	117616
CM-B21-2265	−20.17	Molluscan shell	<i>B. ariakensis</i> Habe	65	4050 ± 50	−1.1	4450 ± 50	117617
CM-B22-2392	−21.44	Molluscan shell	<i>B. tsurumaru</i> Habe	75	4580 ± 50	−1.0	4980 ± 50	117618
CM-B23-2463	−22.15	Molluscan shell	<i>Tellinide</i>	40	5150 ± 50	−4.7	5490 ± 50	117619
CM-B23-2543	−22.95	Molluscan shell	fragments	61	6010 ± 50	−2.1	6390 ± 50	117620
CM-B24-2734	−24.86	Molluscan shell	<i>B. ariakensis</i> Habe	29	7040 ± 50	−1.3	7430 ± 50	117621
CM-B25-2899	−26.51	Molluscan shell	<i>B. ariakensis</i> Habe	24	8400 ± 50	−7.5	8680 ± 50	117622
<i>JS98</i>								
JS-9-970	−5.50	Molluscan shell	<i>Littoraria</i> sp.	88	1640 ± 40	−6.9	1940 ± 40	130637
JS14-1750	−13.30	Molluscan shell	<i>Corbicula</i> sp., <i>Bornopsis</i> sp.	90	3200 ± 40	−8.1	3480 ± 40	130638
JS-16-1987	−15.67	Molluscan shell	<i>Cryptomya</i> sp. cf. <i>C. busoemis</i> Yokoyama, <i>Theora</i> sp. cf. <i>T. fragilis</i> A. Adams	21	2860 ± 40	−4.6	3200 ± 40	130639
JS-17-2169	−17.49	Molluscan shell	<i>Corbicula</i> sp.	89	2890 ± 40	−4.4	3230 ± 40	130640
JS-19-2530	−21.10	Molluscan shell	<i>Pisidium</i> sp.	34	4750 ± 30	−5.8	5070 ± 30	130641
JS-21-2745	−23.25	Molluscan shell	fragments	127	6640 ± 40	−8.2	6920 ± 40	132938
JS-21-2764	−23.44	Molluscan shell	<i>Corbicula</i> sp.	500	6640 ± 60	−8.9	6900 ± 60	130642
JS-22-2857	−24.37	Molluscan shell	<i>Scapharca</i> sp. cf. <i>S. glohosa ursus</i> Tanaka	190	6070 ± 80	−2.5	6440 ± 80	130643
JS-22-2940	−25.20	Molluscan shell	<i>Cryptomya</i> sp. cf. <i>C. busoensis</i> Yokoyama	105	6050 ± 60	−6.2	6360 ± 60	130644
JS-26-3336	−29.16	Molluscan shell	<i>Cryptomya</i> sp. cf. <i>C. busoensis</i> Yokoyama	550	7410 ± 70	−5.1	7740 ± 70	130645
JS-27-3460	−30.40	Molluscan shell	<i>Cryptomya</i> sp. cf. <i>C. busoensis</i> Yokoyama	134	7220 ± 60	−6.4	7530 ± 60	130646
JS-27-3530	−31.10	Molluscan shell	fragments	182	7500 ± 60	−5.9	7810 ± 60	130647
JS-28-3640	−32.20	Molluscan shell	<i>Cryptomya</i> sp. cf. <i>C. busoensis</i> Yokoyama	340	8660 ± 120	−5.9	8970 ± 120	130648
JS-28-3655	−32.35	Molluscan shell	fragments	94	8200 ± 40	−4.1	8540 ± 40	132939
<i>HQ98</i>								
HQ-2-70	5.21	Snail shell	<i>Helicis</i> sp.	42	180 ± 50	−4.6	520 ± 50	130653
HQ-4-470	1.21	Molluscan shell	<i>Bornopsis</i> sp.	116	4120 ± 50	−7.6	4410 ± 50	130654
HQ-5-550	0.41	Molluscan shell	<i>Bornopsis</i> sp.	52	5230 ± 30	−9.0	5490 ± 30	132941
HQ-5-615	−0.24	Molluscan shell	<i>Bornopsis</i> sp.	67	5580 ± 60	−7.1	5870 ± 60	130655
HQ-10-1330	−7.39	Molluscan shell	<i>Corbicula</i> sp.	218	4310 ± 50	−9.1	4570 ± 50	130656
HQ-17-2320	−17.29	Molluscan shell	<i>Theora</i> sp. cf. <i>T. fragilis</i> A. Adams	53	5310 ± 60	−6.4	5620 ± 60	130657
HQ-20-2860	−22.69	Molluscan shell	<i>Cryptomya</i> sp. cf. <i>C. busoensis</i> Yokoyama	139	6830 ± 70	−4.6	7170 ± 70	130658
HQ-21-3012	−24.21	Plant		51	8130 ± 70	−28.4	8080 ± 70	130659

Errors are indicated at the range of  $\pm 1\sigma$ .

terbedded dark-gray sand and mud with few shell fragments. It overlies Unit C with a transitional contact. The unit ranges from 5.75 to 8.60 m in thickness.

Types a, b, c, and d couplets occur in the unit. Type a couplets are common in CM97. Bidirectional ripple laminations occur in sand layers at about 9 m depth in CM97. Type b couplets are observed in JS98 and HQ98. Type c couplets occur intermittently in JS98. Type d couplets are found in the uppermost part of the unit in all cores.

Other sedimentary structures recognized in this unit are well-sorted very fine to fine sand with ripple or parallel laminations. Sands with ripple laminations are recognized from 6.6 to 7.1 m depth in CM97 and from 7.3 to 7.5 m depth in JS98. Sands with parallel laminations are found from 6.0 to 6.3 m depth in HQ98.

Type d couplets indicate that wave currents as well as tidal currents played an important role in

formation of this unit. An upward-fining succession suggests that the energy of wave and tidal currents decreased gradually upward. As the characteristics of sand–mud couplets in this unit are very similar to the lower intertidal to subtidal sediments reported from the present Changjiang delta (Li et al., 2000b), Unit D is interpreted as lower intertidal to subtidal flat facies.

#### 4.2.5. Unit E (upper intertidal flat)

Unit E consists predominantly of Type f couplets. Sand content is less than 10%. The thickness of this unit is less than 2 m. The boundary between Units D and E is transitional.

The sediments of this unit are similar to muddy intertidal flat deposits described by Reineck and Singh (1980). Moreover, this facies is analogous to the present upper intertidal flat sediments in the Changjiang River delta (Li et al., 2000b), Unit E is interpreted as upper intertidal flat facies.

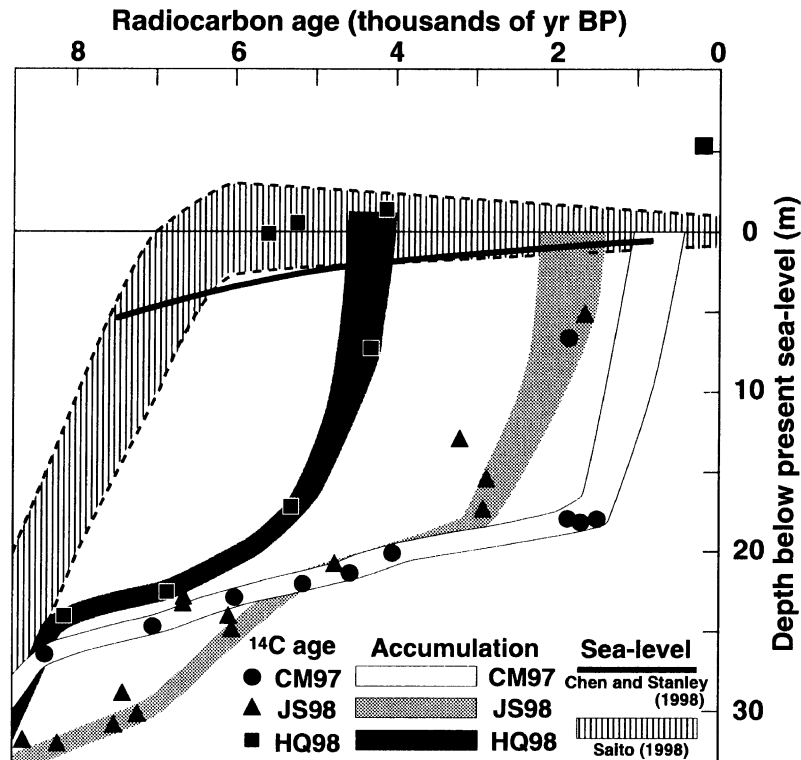


Fig. 5. Accumulation curve for each borehole site and Holocene sea-level curves. Slope of each curve represents the sediment accumulation rate. Sea-level curves are after Saito (1998) for the East China Sea, and Chen and Stanley (1998) for the Tai Lake region, south of the Changjiang delta.

#### 4.2.6. Unit F (surface soil)

Unit F is characterized by dull reddish brown to brown clayey silt, containing abundant plant rootlets and snail shells. Artificial angular tiles were observed in CM97. The thickness of the unit is 0.4 m in CM97, 1.9 m in JS98, and 1.2 m in HQ98. Sand content in most of the unit is < 20%. The lower contact with Unit E is transitional. These characteristics indicate that Unit F is a surface soil.

#### 4.3. $^{14}\text{C}$ ages and sediment accumulation rates

Table 1 summarizes 32  $^{14}\text{C}$  ages obtained from the three boreholes. Fig. 5 shows age-depth plots (accumulation curves) for each site, along with late Quaternary sea-level curves in the Changjiang delta and the East China Sea (Chen and Stanley, 1998; Saito, 1998).  $^{14}\text{C}$  ages from these boreholes reveal that deltaic sediments were deposited beginning about 8000 years BP. Prodelta sediments accumulated over a period of about 5500 years in CM97 and about 1000 years in HQ98. Tidal sand-ridge sediments were deposited from 8700 to ca. 3000 years BP only in JS98. The delta front at 10 m depth passed the HQ98, JS98, and CM97 sites about 4500, 2200, and 1200 years BP, respectively.

We are able to determine sediment accumulation rate by using  $^{14}\text{C}$  ages associated with depositional units. The depositional rate of the prodelta sediments and tidal sand-ridge sediments were about 1.1 and 2.5 m/kyear, respectively. An accumulation rate of > 3.5 m/kyear, was observed in the delta front to lower intertidal to subtidal flat sediments in all cores.

## 5. Discussion

### 5.1. Unit (facies) distribution and sedimentary environment

The longitudinal profile X–Y (Fig. 6) illustrates unit (facies) distribution among the three boreholes. Isochron lines were drawn based on the  $^{14}\text{C}$  dates. The present active delta front is located about 50 km southeast of the present coastline. Deltaic facies, Units B to F, identified in the borehole sediments correspond well with the present-day sedimentary environments of the Changjiang delta (Fig. 1) (De-

partment of Marine Geology, Tongji University, 1975; Li, 1986; Li et al., 2000b). Tidal sand-ridge facies (Unit A) occurs only in JS98. Li et al. (1999) reported that strong tidal currents formed radial tidal sand ridges, whose apex was probably situated near Dongtai, in the western part of the Yellow Sea during early to mid-Holocene. Thus, the JS98 site would be located at its margins, resulting in the lack of prodelta facies (Unit B).

Fig. 7 compares the deltaic facies of this study with previous subsurface works. Our results correlate well with other studies. It is easy to determine the boundary between delta front and prodelta facies (or shallow marine, estuary, neritic) because prodelta facies consists largely of clay and delta front facies consists of sandy deposits. However, the boundary between delta front and delta plain facies is not clear in previous studies. We propose that the change from coarsening-upward to fining-upward successions in core sediments is useful in determining these facies boundaries.

Combined litho- and chronostratigraphic analyses in our study clearly indicate that isochron lines approximating former depositional/topographic surfaces cross unit boundaries. For example, the CM97 site, located approximately 130 km seaward of the HQ98 site, was still a prodelta environment when the HQ98 site was a delta front environment. Depositional rates at the CM97 site were much lower than at the HQ98 site at that time. The grain size of sediments in the prodelta environment at the CM97 site was also significantly finer than in the delta front environment at the HQ98 site because coarser fractions of the sediments supplied by the river were deposited near the river mouth, while finer fractions were transported farther offshore, as is the case at the present. Accumulation rates and grain size changed abruptly when the delta front approached and passed the CM97 site. These facies relationships agree with the delta progradation model proposed by Scruton (1960).

The prodelta sediments in CM97 were thicker than in HQ98. This difference in thickness is thought to be due to a difference in the duration of the prodelta environment at each site because accumulation rates of prodelta sediments at both sites were nearly equal. On the other hand, delta front deposits in HQ98 are thicker than in CM97. Subtidal flat

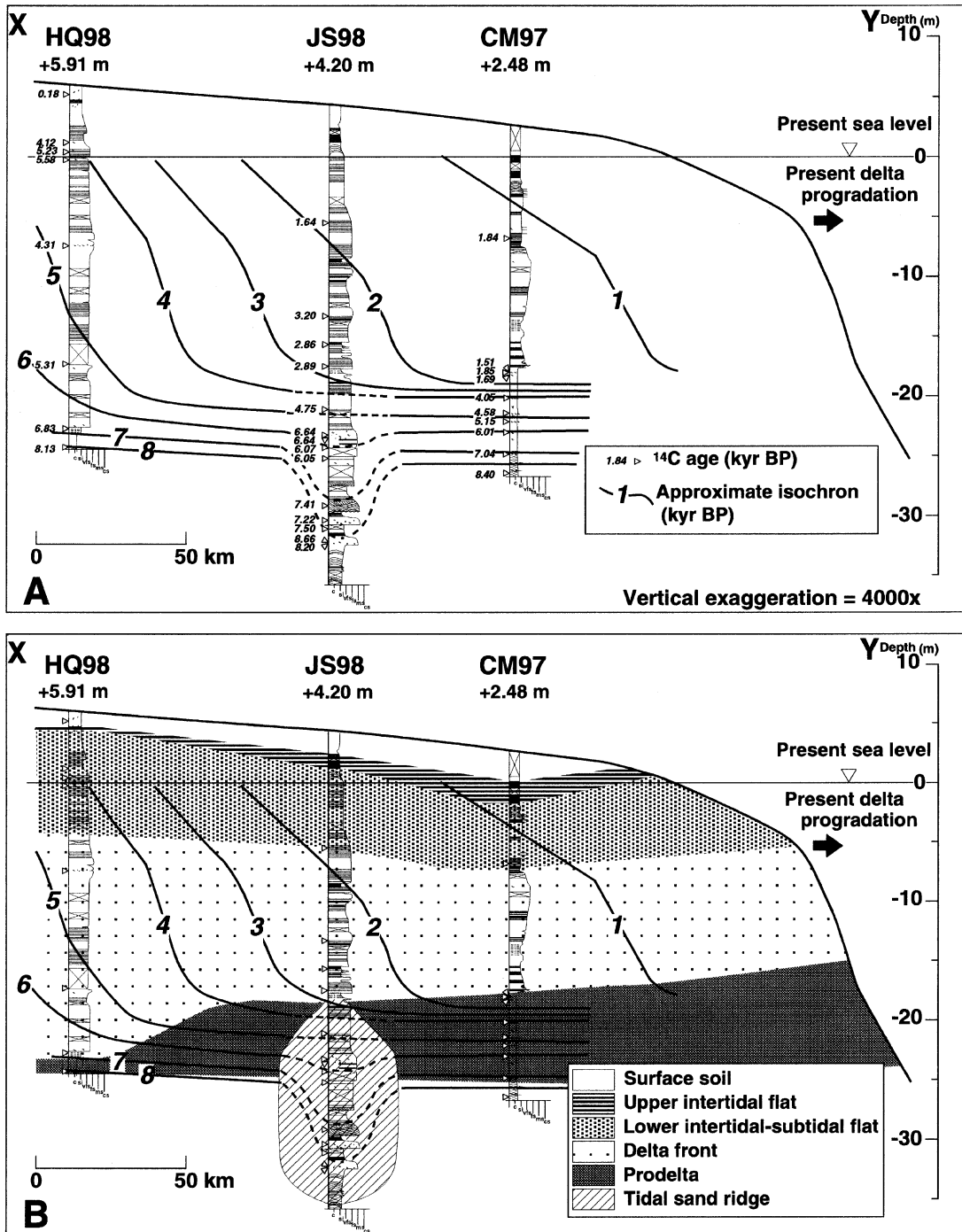


Fig. 6. Stratigraphy of a longitudinal cross section (X–Y). The location is shown in Fig. 1. Each unit is described in the text and summarized in more detail in Fig. 3. Isochron lines are based on  $^{14}\text{C}$  dates and accumulation curves shown in Fig. 5. The altitude of each facies in the CM97 site is lower than that of present, which probably resulted from sediment compaction. The data for recent sedimentary environment of the Changjiang delta are from Department of Marine Geology, Tongji University (1975), Li (1986), and Li et al. (2000b).

This study	Wang et al. (1981)	Li et al. (1979) Li and Li (1983)	Stanley and Chen (1993)	Li et al. (2000a)
Surface soil	Delta plain	Delta plain	Delta plain	Deltaic
Upper intertidal flat				
Lower intertidal to subtidal flat				
Delta front	Delta front	Delta front	Delta front	
Prodelta	Prodelta, Shallow marine, Estuarine (?)	Prodelta- shallow marine, Neritic	Prodelta	Estuary-shallow marine

Fig. 7. Comparative interpretations of the sedimentary facies of the delta deposits (Li et al., 1979).

sediments do not show substantial differences in thickness among the three cores.

The altitude of the top of the upper intertidal flat facies decreased seaward from 4.8 m at HQ98 to 2.4 m at JS98 to 0.1 m at CM97. This level must be lower than the high-tide level, and two different explanations for this phenomenon are possible. The sea level could have been higher than the present level during the mid-Holocene, falling slightly since then. The other possible explanation is that the tidal range has become smaller because of the infilling of the funnel-shaped bay caused by the progradation of the Changjiang delta. However, the amplitude of the tidal range or of tidal influence has not changed greatly because the total thickness of the intertidal and subtidal sediments was almost the same among the three sites. Therefore, a fall in sea level since the mid-Holocene caused by hydro-isostasy after deglaciation is a better explanation (Nakada et al., 1991). The difference in sea-level curves obtained in the coastal area of the south part of the Changjiang delta (Chen and Stanley, 1998) might also result from the effect of hydro-isostasy on different locations in these areas.

### 5.2. Delta progradation rates

The delta front has prograded more than 250 km since 6000 years BP at an average rate of about 50 km/kyear. However, the rate was not constant, and changed abruptly in the late Holocene. The progradation rate increased suddenly about 2000 years BP, when it went from 38 to 80 km/kyear (Figs. 6 and 8a). This change to a rapid progradation rate can be correlated with the active extension of the subaerial delta plain described by Wang et al. (1981) (Fig. 8b).

The rapid growth of the southern part of the subaerial delta, where cheniers have developed, probably occurred at the same time (Fig. 8c, d) (Wang et al., 1981; Chen, 1996, 1998; Chen et al., 1985a). The increase of progradation rates would reflect the change in sediment discharge to the lower reaches and the delta area because deltaic deposits show little variation in thickness in the longitudinal profile. Therefore, sediment discharge in the lower reaches after 2000 years BP must have been almost double the amount of discharge before 2000 years BP.

The shoreline at the river mouth was more of a funnel or estuarine shape around 2000 or 3000 years BP than now (Chen et al., 1985a). Thus, the direction of progradation after about 2000 years BP might not have been regular, but could have changed from eastward to southeastward because of (1) the Coriolis effect (Li and Li, 1983); (2) subsidence near the present river mouth (Stanley and Chen, 1993; Chen and Stanley, 1995); (3) the influence of longshore currents, or any combination of these influence. If the principal direction of progradation shifted from eastward to southeastward, recent sediment discharge to the lower reaches and delta area must be much larger than the above estimate.

Several causes are considered for the active progradation. An increase in sediment production in the drainage basin could have occurred due to widespread human activities (Chen et al., 1985a). First, rice domestication had already begun along the middle reaches in the early Holocene (Zhao, 1998). The pollen record from Poyang Lake in the middle reaches suggests that human-induced vegetational change and the expansion of intensive rice agriculture into the dryland forests had occurred after about 2000 years BP (Jiang and Piperno, 1999). Furthermore, Jarvis (1993) has reported that human distur-

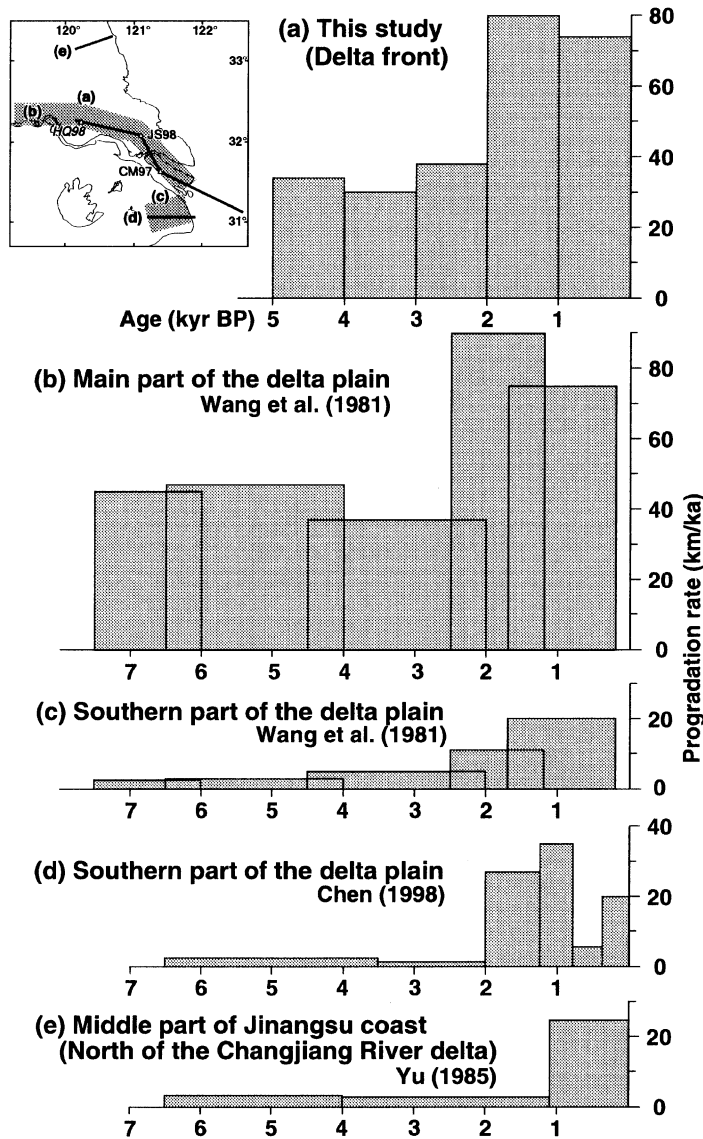


Fig. 8. Progradation rates of the Changjiang delta and the middle part of the Jiangsu coast, north of the Changjiang delta. Data are compiled from Wang et al. (1981), Yu (1985), and Chen (1998). (b) and (c) are represented by dark shaded zone because Wang et al. (1981) did not show exact location of their projection lines.

bance increased in Sichuan Province located in the upper reaches of the river after about 1000 years BP. Therefore, active human influence could have increased sediment production in the drainage basin after about 2000 years BP. In China, extensive agri-

cultural use of the loess plateau within the Yellow River drainage basin has also resulted in significant increase in sediment discharge to the ocean after about 200 BC (Ren and Shi, 1986; Milliman et al., 1987; Saito et al., 2001).

The other possible cause is a relative decrease in deposition in the middle reaches related to increased river-channel stability. The middle reaches of the Changjiang extend 927 km from Yichang to Hukou and are characterized by extensive flood plains and a large number of natural lakes, such as Dongting and Poyang Lakes. The longitudinal gradient of the river bed in the middle reaches is low, with a mean value of approximately 0.00003 (Chen, 1996). Even now, the middle reaches are subject to heavy flooding frequent during the rainy season, and about 20% of the sediment discharge measured at Yichang station is deposited in Dongting Lake, located downstream from the station (Shi et al., 1985). Chen et al. (2001) also demonstrates that at least one-third of the sediment load that passes through the station is trapped in the middle reaches. It is possible that climatic cooling after the mid-Holocene (Winkler and Wang, 1993) and human activity, such as dike construction, might have decreased the flooding in the middle reaches, resulting in relative increase in sediment discharge to the delta area.

The shift of the mouth of the Yellow River did not directly influence this phenomenon because from AD 1128 to 1855, the Yellow River emptied into the Yellow Sea in Jiangsu Province, about 300 km north of the present Changjiang River mouth. Progradation rates on the coastal plain of Jiangsu Province clearly increased during the last 1000 years, related to the sediment supply from the old Yellow River (Yu, 1985) (Fig. 8e). As the rapid progradation of the Changjiang delta occurred about 1000 years before the Yellow River course shift, the sediment supply from the Yellow River was not a direct cause of that change.

## 6. Conclusions

Three radiocarbon-dated borings clarify the sediment characteristics and architecture of the Changjiang River delta in detail and show the subaqueous delta progradation quantitatively. The main results of this study are as follows.

(1) The delta succession was classified into five facies, which were interpreted as prodelta, delta front, subtidal to lower intertidal flat, upper intertidal flat, and surface soil, in ascending order. The prodelta to

delta front facies show an upward-coarsening succession, which was covered by an upward-fining succession from the uppermost part of the delta front to the surface soil.

(2) Very thinly interbedded to thinly interlaminated sand and mud (sand–mud couplets) and bidirectional ripple laminations occur commonly in the deltaic sediments, resulting from strong tidal influence.

(3) Sediment accumulation rate was about 1.1 m/kyear in prodelta sediments, but > 3.5 m/kyear in the delta front to lower intertidal to subtidal flat sediments.

(4) Delta progradation had already begun at 6000 years BP. Although the average rate for the last 5000 years was about 50 km/kyear, progradation rate increased abruptly from 38 to 80 km/kyear after about 2000 years BP. Possible causes are increase in sediment production in the drainage basin due to the widespread human influence and/or the relative decrease in deposition in the middle reaches related to increased river-channel stability.

## Acknowledgements

We would like to thank Prof. Zhongyuan Chen for encouraging us to submit a paper to this special issue and for his kind reviews of the manuscript. Dr. Andrew G. Warne provided many helpful suggestions during the review stage. We thank staff of the Department of Marine Geology, Tongji University for their support, and Messers Toshifumi Komatsu, Basara Miyahara, and Susumu Tanabe for their assistance in sampling. This research was funded by the Global Environment Research Fund of the Ministry of the Environment, Japan, and in part by a Grant-in-aid from the Scientific Research Project (Project Number 10-5088) of the Ministry of Education, Culture, Sports, Science and Technology, Japan. K.H. thanks the Japan Society for the Promotion of Science for a research fellowship.

## References

- Chen, X., 1996. An integrated study of sediment discharge from the Changjiang River, China, and the delta development since the mid-Holocene. *J. Coastal Res.* 12, 26–37.

- Chen, X., 1998. Changjiang (Yangtze) River delta, China. *J. Coastal Res.* 14, 838–858.
- Chen, Z., 1999. Geomorphology and coastal changes of the lower Yangtze delta plain, China. In: Miller, A.J., Gupta, A. (Eds.), *Varieties of Fluvial Form*. Wiley, Chichester, pp. 428–443.
- Chen, Z., Stanley, D.J., 1995. Quaternary subsidence and river channel migration in the Yangtze Delta Plain, Eastern China. *J. Coastal Res.* 11, 927–945.
- Chen, Z., Stanley, D.J., 1998. Sea-level rise on eastern China's Yangtze delta. *J. Coastal Res.* 14, 360–366.
- Chen, J., Zhu, S., Lu, Q., Zhou, Y., He, S., 1982. Descriptions of the morphology and sedimentary structures of the river mouth bar in the Changjiang estuary. In: Kennedy, V.S. (Ed.), *Estuarine Comparisons*. Academic Press, New York, pp. 667–676.
- Chen, J., Zhu, H., Dong, Y., Sun, J., 1985a. Development of the Changjiang estuary and its submerged delta. *Cont. Shelf Res.* 4, 47–56.
- Chen, Y., Peng, G., Jiao, W., 1985b. Radiocarbon dates from the East China Sea and their geological implications. *Quat. Res.* 24, 197–203.
- Chen, Z., Zhou, C., Yang, W., Wu, Z., 1987. Subaqueous topography and sediments off modern Changjiang Estuary. In: Yan, Q., Xu, S. (Eds.), *Recent Yangtze Delta Deposits*. East China Normal Univ. Press, Shanghai, pp. 238–245 (in Chinese with English abstract).
- Chen, Z., Li, J.F., Shen, H.T., 2001. Yangtze River of China: historical analysis of discharge variability and sediment flux. *Geomorphology* 41 (2–3), 77–91.
- Coleman, J.M., 1981. *Deltas: Processes of Deposition and Models for Exploration*. Burgess Publishing, Minneapolis, 124 pp.
- Coleman, J.M., Wright, L.D., 1975. Modern river deltas: variability of processes and sand bodies. In: Broussard, M.L. (Ed.), *Deltas, Models for Exploration*. Houston Geological Society, Houston, TX, pp. 99–149.
- Davis, R.A., Hayes, M.O., 1984. What is a wave-dominated coast? *Mar. Geol.* 60, 313–329.
- Department of Marine Geology, Tongji University, 1975. *Basic Characteristics of Modern Sedimentation in the Changjiang Delta*. Tongji University, Shanghai, 61 pp. (in Chinese).
- Editorial Board for Marine Atlas, 1990. *Marine Atlas of Bohai Sea, Yellow Sea, East China Sea*. Geology and Geophysics, China Ocean Press, Beijing (in Chinese).
- Galloway, W.E., 1975. Process framework for describing the morphologic and stratigraphic evolution of deltaic depositional systems. In: Broussard, M.L. (Ed.), *Deltas, Models for Exploration*. Houston Geological Society, Houston, TX, pp. 87–98.
- Houbolt, J.J.H.C., 1968. Recent sediments in the southern bight of the North Sea. *Geol. Mijnbouw* 47, 245–273.
- Jarvis, D.I., 1993. Pollen evidence of Changjiang Holocene monsoon climate in Sichuan Province, China. *Quat. Res.* 39, 325–337.
- Jiang, Q., Piperno, D.R., 1999. Environmental and archeological implications of a Late Quaternary palynological sequence, Poyang Lake, southern China. *Quat. Res.* 52, 250–258.
- Lee, H.J., Yoon, S.H., 1997. Development of stratigraphy and sediment distribution in the northeastern Yellow Sea during Holocene sea-level rise. *J. Sediment. Res.* 67, 341–349.
- Li, C., 1986. Deltaic sedimentation. In: Ren, M. (Ed.) *Modern Sedimentation in Coastal and Nearshore Zone of China*. China Ocean Press, Beijing and Springer Verlag, Berlin, pp. 253–378.
- Li, C., Li, P., 1983. The characteristics and distribution of Holocene sand bodies in the Changjiang delta area. *Acta Oceanol. Sin.* 2, 54–66.
- Li, C., Guo, X., Xu, S., Wang, J., Li, P., 1979. The characteristics and distribution of Holocene sand bodies in Changjiang River delta area. *Acta Oceanol. Sin.* 1, 252–268 (in Chinese with English abstract).
- Li, C., Li, P., Cheng, X., 1983. The influence of marine factors on sedimentary characteristics of Yangtze River channel below Zhenjiang. *Acta Geogr. Sin.* 38, 128–140 (in Chinese with English abstract).
- Li, C., Zhang, J., Yang, S., Fan, D., 1999. Characteristic and paleoenvironmental evolution of subaerial tidal sand body in Subei coastal plain. *Sci. China, Ser. D: Earth Sci.* 42, 52–60.
- Li, C., Chen, Q., Zhang, J., Yang, S., Fan, D., 2000a. Stratigraphy and paleoenvironmental changes in the Yangtze delta during Late Quaternary. *J. Asian Earth Sci.* 18, 63–79.
- Li, C., Wang, P., Fan, D., Dang, B., Li, T., 2000b. Open coast intertidal deposits and their preservation potential: a case study from east-central China. *Sedimentology* 47, 1039–1051.
- Liu, C., Walker, H.J., 1989. Sedimentary characteristics of cheniers and the formation of the chenier plains of East China. *J. Coastal Res.* 5, 353–368.
- Liu, Z., Huang, Y., Zhang, Q., 1989. Tidal current ridges in the southwestern Yellow Sea. *J. Sediment. Petrol.* 59, 432–437.
- Liu, K., Sun, S., Jiang, X., 1992. Environmental change in the Yangtze River delta since 12,000 years BP. *Quat. Res.* 38, 32–45.
- Milliman, J.D., 1991. Flux and fate of fluvial sediment and water in coastal seas. In: Montoura, R.F.C., Martin, J.-M., Wollast, R. (Eds.), *Ocean Margin Processes in Global Change*. Wiley, Chichester, pp. 69–89.
- Milliman, J.D., Meade, R.H., 1983. World-wide delivery of river sediment to the oceans. *J. Geol.* 91, 1–21.
- Milliman, J.D., Syvitski, J.P.M., 1992. Geomorphic/tectonic control of sediment discharge to the oceans: the importance of small mountain rivers. *J. Geol.* 100, 525–544.
- Milliman, J.D., Qin, Y., Ren, M., Saito, Y., 1987. Man's influence on the erosion and transport of sediment by Asian rivers: the Yellow River (Huanghe) example. *J. Geol.* 95, 751–762.
- Nakada, M., Yonekura, N., Lambeck, K., 1991. Late Pleistocene and Holocene sea-level changes in Japan: implications for tectonic histories and mantle rheology. *Palaeogeogr., Palaeoclimatol., Palaeoecol.* 85, 107–122.
- Orton, G.J., Reading, H.G., 1993. Variability of deltaic processes in terms of sediment supply, with particular emphasis on grain size. *Sedimentology* 40, 475–512.
- Park, S.C., Lee, S.D., 1994. Depositional patterns of sand ridges in tide-dominated shallow water environments: Yellow Sea coast and South Sea of Korea. *Mar. Geol.* 120, 89–103.
- Reineck, H.E., Singh, I.B., 1980. *Depositional Sedimentary Environments*. Springer-Verlag, New York, 549 pp.
- Reineck, H.E., Wunderlich, F., 1968. Classification and origin of flaser and lenticular bedding. *Sedimentology* 11, 99–104.

- Ren, M., Shi, Y., 1986. Sediment discharge of the Yellow River (China) and its effect on the sedimentation of the Bohai and the Yellow Sea. *Cont. Shelf Res.* 6, 785–810.
- Saito, Y., 1998. Sea levels of the last glacial in the East China Sea continental shelf. *Quat. Res. (Daiyonki Kenkyu)* 37, 237–242 (in Japanese with English abstract).
- Saito, Y., Yang, Z., Hori, K., 2001. The Huanghe (Yellow River) and Changjiang (Yangtze River) deltas: a review on their characteristics, evolution and sediment discharge during the Holocene. *Geomorphology* 41 (2–3), 219–231.
- Scruton, P.C., 1960. Delta building and the deltaic sequence. In: Shepard, F.P., van Andel, T.H. (Eds.), *Recent Sediments, Northwest Gulf of Mexico*. Am. Assoc. Petrol. Geol., Tulsa, OK, pp. 82–102.
- Shen, H., 1998. Material flux and land-and-ocean interactions in the Changjiang (Yangtze) estuary. In: Saito, Y., Ikehara, K., Katayama, H. (Eds.), *Proceedings of an International Workshop on Sediment Transport and Storage in Coastal Sea-Ocean System*. STA (JISTEC) and Geological Survey of Japan, Tsukuba, pp. 1–7.
- Shen, H., Guo, C., Zhu, H., Xu, H., Yun, C., Chen, B., 1988. A discussion on the change and origin of turbidity maximum in the Changjiang Estuary. In: Chen, J., Shen, H., Yu, C. (Eds.), *Process of Dynamics and Geomorphology of the Changjiang Estuary*. Shanghai Scientific and Technical Publishers, Shanghai, pp. 216–228 (in Chinese).
- Shi, Y., Yang, W., Ren, M., 1985. Hydrological characteristics of the Changjiang and its relation to sediment transport to the sea. *Cont. Shelf Res.* 4, 5–15.
- Stanley, D.J., 1988. Subsidence in the northeastern Nile delta: rapid rates, possible causes, and consequences. *Science* 240, 497–500.
- Stanley, D.J., Chen, Z., 1993. Yangtze delta, eastern China: 1. Geometry and subsidence of Holocene depocenter. *Mar. Geol.* 112, 1–11.
- Stanley, D.J., Chen, Z., 1996. Neolithic settlement distributions as a function of sea level-controlled topography in the Yangtze delta, China. *Geology* 24, 1083–1086.
- Stanley, D.J., Warne, A.G., 1994. Worldwide initiation of Holocene marine deltas by deceleration of sea-level rise. *Science* 265, 228–231.
- Wang, J., Guo, X., Xu, S., Li, P., Li, C., 1981. Evolution of the Holocene Changjiang delta. *Acta Geol. Sin.* 55, 67–81 (in Chinese with English abstract).
- Winkler, M.G., Wang, P.K., 1993. The Late Quaternary vegetation and climate of China. In: Wright Jr., H.E., Kutzbach, J.E., Webb III, T., Ruddiman, W.F., Street-Perrott, F.A., Bartlein, P.J. (Eds.), *Global Climates Since the Last Glacial Maximum*. Univ. Minnesota Press, Minnesota, pp. 221–264.
- Xu, S., Shao, X., Chen, Z., Yan, Q., 1990. Storm deposits in the Changjiang Delta. *Sci. China, Ser. B* 33, 1242–1250.
- Yan, Q., Xu, S., Shao, X., 1989. Holocene cheniers in the Yangtze delta, China. *Mar. Geol.* 90, 337–343.
- Yu, Z., 1985. On the formation of beach ridges in middle part of Jiangsu, East China. *Trans. Jpn. Geomorphol. Union* 6, 351–359 (in Japanese with English abstract).
- Zhao, Z., 1998. The Middle Yangtze region in China is one place where rice was domesticated: phytolith evidence from the Diaotonghuan Cave, Northern Jiangxi. *Antiquity* 72, 885–897.
- Zhao, X., Geng, X., Zhang, J., 1979. Sea level changes of the eastern China during the past 20,000 years. *Acta Oceanol. Sin.* 1, 269–281 (in Chinese with English abstract).
- Zhu, H., Yun, C., Mao, Z., Wang, S., 1988. Characteristics and empiric relationships of wind generated wave in the Changjiang estuary. In: Chen, J., Shen, H., Yu, C. (Eds.), *Process of Dynamics and Geomorphology of the Changjiang Estuary*. Shanghai Scientific and Technical Publishers, Shanghai, pp. 166–177 (in Chinese).